Near-white light-emitting Dy^{3+}-doped transparent glass ceramics containing Ba_2LaF_7 nanocrystals

Shaoye Ouyang (欧阳绍业), Weihuan Zhang (张为欢), Zhixiong Zhang (张志雄), Yuepin Zhang (张约品)*, and Haiping Xia (夏海平)

Key Laboratory of Photo-Electronic Material, Ningbo University, Ningbo 315211, China
**Corresponding author: zhangyuepin@nbu.edu.cn*

Received April 18, 2015; accepted June 8, 2015; posted online July 14, 2015

Glass ceramics Ba_2LaF_7:xDy^{3+} are obtained through the conventional melt-quenching technique, and their luminescent properties are investigated. Under 350 nm excitation, the emission spectra consists of a strong blue-yellow band as well as a weak red emission centered at 660 nm, which are attributed to the $^4F_{9/2} \rightarrow {}^6H_{15/2}$, $^4F_{9/2} \rightarrow {}^6H_{13/2}$ and $^4F_{9/2} \rightarrow {}^6H_{11/2}$ transitions of the Dy^{3+} ion, respectively. The corresponding Commission Internationale de L'Eclairage (CIE) chromaticity coordinate for a sample of 2 mol.% Dy_2O_3 after being heat-treated at 690°C is (0.313, 0.328). It is concluded that the formed materials may have the possibility of applications for white light-emitting diodes (LEDs).

OCIS codes: 160.2540, 160.4760, 160.5690.
doi: 10.3788/COL201513.091601.

Up to now, white light-emitting diodes (LEDs) have obtained more and more attention and turned out to be a welcomed substitution for conventional incandescent and fluorescent lamps, owing to their advantages of great brightness, excellent reliability, eco-friendliness, and their outstanding characteristics of energy conservation[1]. Conventionally, it is of great help to generate the white light to make a combination of YAG:Ce^{3+} phosphor and blue InGaN chip or just to connect the RGB phosphors with a near-UV (350–410 nm) LED chip[2,3]. Despite the achievements in developing white LEDs, it is also essential to figure out their existing drawbacks. On the one hand, YAG:Ce^{3+} phosphors pumped by blue chips have the disadvantages of a low color rendering index and the instability of the obtained white light, which results in poor color rendering[4,5]. On the other hand, the combination of tri-color phosphors seems to be unrealistic for near-UV LED chips on account of a fact that the large Stokes shift between excitation and emission in the UV-excitable phosphor may decrease the luminous efficiency[6]. Hence, there is an urgent need to explore a more promising candidate for white LEDs.

It is worth mentioning that glass ceramics have recently been studied for the fabrication of white LEDs. Not only does a glass ceramic have the advantages of glass, but it is also in possession of the excellent properties originating from the precipitated crystalline phase in the glassy matrix. In addition, rare earth-doped glass ceramics have the merits of effective luminescence, plain manufacturability, and a remarkable heat-resistant quality[7–11].

Among rare earth ions, Dy^{3+} ions have been considered to be the most adaptable selection for analyzing luminescence properties, and it is known that the visible luminescence of the Dy^{3+} ion is mainly composed of the characteristic blue emission band (470–500 nm) and the yellow emission band (570–600 nm), which corresponds to the $^4F_{9/2} \rightarrow {}^6H_{15/2}$ and $^4F_{9/2} \rightarrow {}^6H_{13/2}$ transitions, respectively. Due to the possible combinations of emitted blue and yellow light to generate white light, the luminescent materials doped with Dy^{3+} ions have been paid more attention and are expected to achieve their potential applications in white LEDs. Though only a few investigations on rare earth-doped crystals or glass ceramics for white LEDs have been carried out, like $K_3Gd(PO_4)_2$:Tb^{3+}[12], there are still no articles about the luminescence properties of Ba_2LaF_7:Dy^{3+}. This work reports the formation of Dy^{3+} ion-doped glass ceramics containing Ba_2LaF_7 nanocrystals, which occupy the intense blue and yellow emission ranges, as well as a weak red emission range. The results favor the development of white LEDs.

Samples of $48SiO_2$–$12AlF_3$–$4TiO_2$–$(30–x)BaF_2$–$6LaF_3$ (mol.%) and x mol.% Dy_2O_3 ($x = 1, 2, 4$) were prepared by the conventional method of melt-quenching. SiO_2, AlF_3, TiO_2, BaF_2, LaF_3, and Dy_2O_3 were used as the raw materials and were of great purity (99.99%). Then, all the starting proportions are mixed systematically and placed into a small quartz crucible, which was prepared for being melted in a furnace at 1450°C for 2 h in the ambient atmosphere. The obtained formations were poured onto a steel plate and annealed in a muffle furnace at 500°C for 2 h to release the inner stress until it at last cooled down to room temperature. With the purpose of investigating transparent glass ceramics, the samples were heat-treated at 640°C for 2 h and denoted as 1GC640, 2GC640, and 4GC640. Also, the materials with the 2 mol.% concentration of Dy^{3+} ions need to be heated at 660°C and 690°C and marked as 2GC660 and 2GC690, respectively. The precursor glass of the 2 mol.% Dy_2O_3 was marked as 2PG. After these procedures, the specimens were cut and polished to plates of about 20 mm × 20 mm × 4 mm in size for the required measurements.

Differential scanning calorimetry (DSC) was performed using a Q2000 DSC (TA Instruments, USA) with 10 mg PG specimen under an N_2 atmosphere at a heating rate of 10°C/min. The crystalline phases of the specimens were identified by X-ray diffraction (XRD), which was measured using an XD-98X diffractometer (XD-3, Beijing) with a Cu tube and $K\alpha$ radiation at 1.54030 Å. The scanning 2θ was from 10° to 90° with 0.02° increments and a 6 s sweep time. The microstructures of the glass and glass ceramics were analyzed by a JEOL2100 microscope with an accelerating voltage of 200 kV. The absorption spectra were measured by a Perkin-Elmer Lamda35 spectrometer. The excitation and emission spectra were measured by a Hitachi F-4500 spectrometer with a Xe lamp as an excitation light source. The luminescence decay was measured using a microsecond flash-lamp as the excitation source. All of the measurements were carried out at room temperature.

Figure 1 depicts the DSC curve of the prepared $48SiO_2$–$12AlF_3$–$4TiO_2$–$28BaF_2$–$6LaF_3$–$2Dy_2O_3$ glass. The temperature of the glass transition and initial crystallization are around 595°C and 665°C, respectively. The crystallization peaks denoted as T_{c1} (740°C) stands for the precipitation of the Ba_2LaF_7 nanocrystals in the glassy matrix. Accordingly, it is reasonable to select 500°C as the annealed temperature and 640°C, 660°C, and 690°C as the heat-treated temperatures for the deposition of the Ba_2LaF_7 nanocrystals.

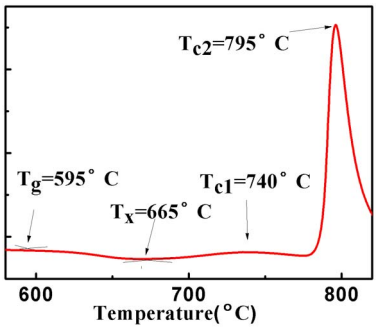

Fig. 1. DSC curve of the prepared $48SiO_2$–$12AlF_3$–$4TiO_2$–$28BaF_2$–$6LaF_3$–$2Dy_2O_3$ glass.

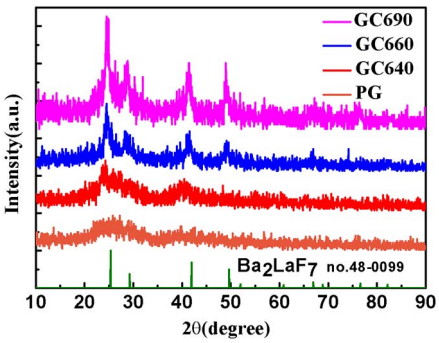

Fig. 2. The XRD patterns of the glass and glass ceramics with a 2 mol.% concentration of Dy_2O_3.

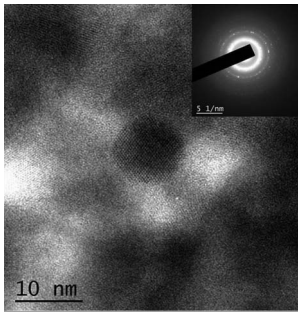

Fig. 3. The TEM image of 2GC690. The inset shows the corresponding SAED patterns.

Figure 2 shows the XRD patterns of the glass and glass ceramics with a 2 mol.% concentration of Dy_2O_3. With the heat-treated temperature rising up from 640°C to 690°C, the corresponding diffraction peaks appear and become more intense and sharp, which also coincides well with the standard XRD data of Ba_2LaF_7 (PDF No. 48-0099). This clearly demonstrates that the Ba_2LaF_7 phase has been formed in the glassy base.

The transmission electron microscopy (TEM) image of 2GC690 is presented in Fig. 3, and the inset provides the selected area electron diffraction (SAED) patterns. As can be seen from Fig. 3, the distributed grain confirms the formation of Ba_2LaF_7 nanocrystals, which corresponds to the results revealed in the XRD patterns. Furthermore, the inset indicates the crystalline state of the obtained nanoparticles.

Figure 4(a) shows the transmission spectra of the samples heated at 640°C with different additions of Dy^{3+} ions in the wavelength region of 300–800 nm. It can be observed that the transparency of these glass ceramics remains at a high level of 70%–80%. Additionally, the intensity of the absorption peaks increases when promoting the concentration of Dy_2O_3 to 2 mol.%, but decreases at 4 mol.%. This implies that the optimum doping content of Dy_2O_3 in glass ceramics containing Ba_2LaF_7 nanocrystals is definitely around 2 mol.%. The transmission spectra of the glass and glass ceramics with 2 mol.% Dy_2O_3 are given in the Fig. 4(b). After the heat treatment, the transmittance of the samples is slightly weakened compared

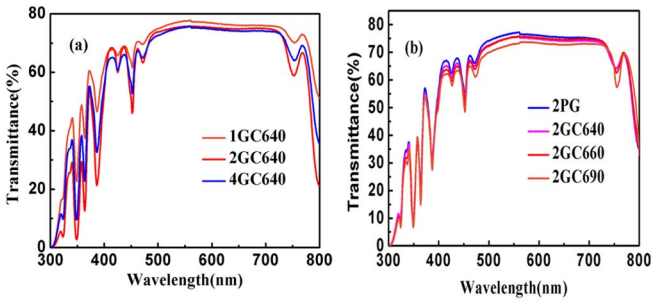

Fig. 4. (a) The transmission spectra of 1GC640, 2GC640, and 4GC640. (b) The transmission spectra of 2PG, 2GC640, 2GC660, and 2GC690.

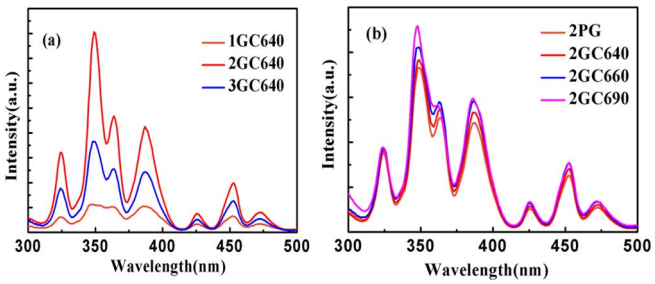

Fig. 5. (a) The excitation spectra of 1GC640, 2GC640, and 4GC640 for 574 nm. (b) The excitation spectra of 2PG, 2GC640, 2GC660, and 2GC690 for 574 nm.

with the precursor glass, but still presents a decent level, which may be ascribed to the smaller size of the precipitated Ba_2LaF_7 nanocrystals in comparison with the wavelength of the optical light[13].

Figure 5(a) gives the excitation spectra of glass ceramics with various concentrations of Dy^{3+} ions monitored at 574 nm. The sample with 2 mol.% Dy_2O_3 reaches the maximum value of excitation intensity. In the scope of 300–500 nm, there are several separate excitation bands situated at 324, 350, 364, 387, 425, 453, and 473 nm, which can be assigned to the transitions $^6H_{15/2} \rightarrow {}^6P_{3/2}$, $^6H_{15/2} \rightarrow {}^6P_{7/2}$, $^6H_{15/2} \rightarrow {}^4D_{5/2}$, $^6H_{15/2} \rightarrow {}^4M_{21/2}$, $^6H_{15/2} \rightarrow {}^4G_{11/2}$, $^6H_{15/2} \rightarrow {}^4I_{15/2}$, and $^6H_{15/2} \rightarrow {}^4F_{9/2}$ of the Dy^{3+} ion, respectively[14]. Among these excitation bands, the one at 350 nm ($^6H_{15/2} \rightarrow {}^6P_{7/2}$) reaches the highest value and is in accordance with the wavelength range of the near-UV LEDs. Figure 5(b) shows the excitation spectra for 2PG, 2GC640, 2GC660, and 2GC690. Clearly, there are no distinct changes observed on the places and profiles of those excitation bands. Compared with the precursor glass, the slender growth of the excitation intensity for the glass ceramics could be ascribed to the precipitation of the Ba_2LaF_7 nanocrystals in the host matrix.

Under the 350 nm excitation, the emission spectra of the different concentrations of Dy_2O_3 in the glass ceramics heated at 640°C is shown in Fig. 6(a), and that of glass and glass ceramics with 2 mol.% Dy_2O_3 after the 640°C, 660°C, and 690°C treatments are given in Fig. 6(b). It can be found that all of the emission spectra consist of a blue light and yellow light, as well as a very weak red light, located at 482 nm ($^4F_{9/2} \rightarrow {}^6H_{15/2}$), 573 nm ($^4F_{9/2} \rightarrow {}^6H_{13/2}$), and 661 nm ($^4F_{9/2} \rightarrow {}^6H_{11/2}$), respectively[15]. Despite the impacts of the red emission, there exists a tremendous possibility to adjust the emission intensity ratio of the yellow to blue light in order to obtain the white light under near-UV excitation. Accordingly, the luminescent intensity of the samples gets more intense when increasing the Dy_2O_3 concentration from 1 to 2 mol.%, and decreases at the concentration of 4 mol.% Dy_2O_3. This decrease is caused by the concentration-quenching effects of the Dy^{3+} ions. This indicates that the optimum concentration of Dy_2O_3 may be around the 2 mol.%. Meanwhile, the luminescent intensity of the samples with 2 mol.% Dy_2O_3 becomes slightly stronger when the heat-treated temperature increases from 640°C to 690°C, which can be ascribed to the formation of Ba_2LaF_7 nanocrystals, which results in the homogeneous dispersion of Dy^{3+} in the glassy matrix. The corresponding CIE diagram is depicted in Fig. 7, and the color coordinates are (0.286, 0.291) and (0.313, 0.328) for 2PG and 2GC690, respectively. (0.313, 0.328) of the glass ceramics with 2 mol.% Dy_2O_3 treated at 690°C is very near to the normal white light (0.333, 0.333). Therefore, the obtained material has the feasibility to be applied to white LEDs under near-UV excitation.

Figures 8(a) and 8(b) present the decay curves of 1GC640 and 2GC640 under 350 nm excitation for 482 and 583 nm, respectively. With the concentration of

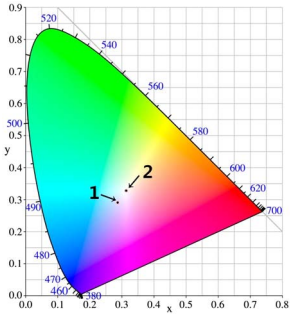

Fig. 7. The chromaticity coordinates of 2PG and 2GC690 under 350 nm excitation (points 1 and 2, respectively).

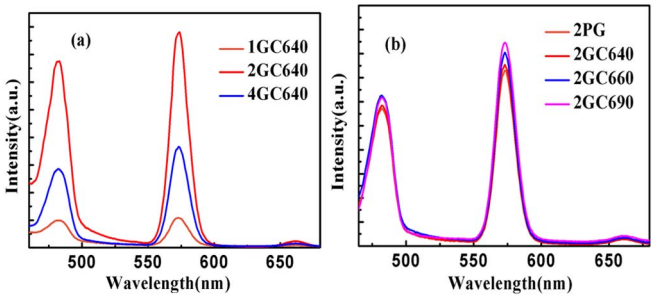

Fig. 6. (a) The emission spectra of 1GC640, 2GC640, and 4GC640 under 350 nm excitation. (b) The emission spectra of 2PG, 2GC640, 2GC660, and 2GC690 under 350 nm excitation.

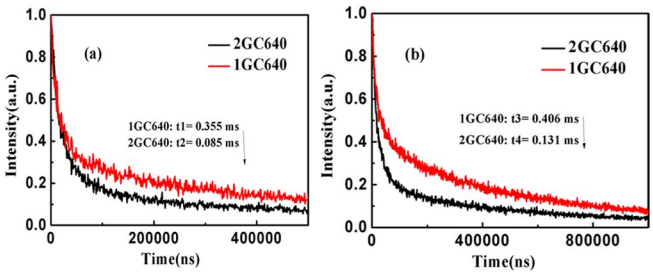

Fig. 8. (a) The decay curves of 1GC640 and 2GC640 under 350 nm excitation for 482 nm. (b) The decay curves of 1GC640 and 2GC640 under 350 nm excitation for 583 nm.

Dy^{3+} up to 2 mol.%, the corresponding lifetime of the $^4F_{9/2} \rightarrow {}^6H_{15/2}$ transition falls down from 0.355 to 0.085 ms, and that of the $^4F_{9/2} \rightarrow {}^6H_{13/2}$ transition also decreases from 0.406 to 0.131 ms. The distance between Dy^{3+} ions may become smaller with the higher content of Dy^{3+} ions in the glassy matrix. Thus, a non-radiative relaxation process that brings about the drop in lifetimes at the $^4F_{9/2}$ level definitely exists. On the one hand, this lifetime quenching could be due to the resonant energy transfer from the excited $^4F_{9/2}$ energy state to nearby Dy^{3+} ion in the $^6H_{15/2}$ ground state, which relies on the distance between the interacting ions. On the other hand, the enhanced possibility of cross-relaxation between a donor (excited Dy^{3+} ion) and an acceptor (ground Dy^{3+} ion) may account for this phenomenon of self-quenching[16–18].

In conclusion, the transparent glass ceramics containing Ba_2LaF_7 nanocrystals with diverse concentrations of Dy^{3+} ion are synthesized, and their luminescent properties are examined. The results show that the optimum concentration of Dy^{3+} ions is around 2 mol.%. Under 350 nm excitation, the emission bands assigned to the $^4F_{9/2} \rightarrow {}^6H_{15/2}$, $^4F_{9/2} \rightarrow {}^6H_{13/2}$, and $^4F_{9/2} \rightarrow {}^6H_{11/2}$ transitions of the Dy^{3+} ion are observed. In addition, the CIE color coordinates for samples with a 2 mol.% Dy^{3+} content is (0.313, 0.328), which is exactly located at the stated region of white light. This gives us the idea that the obtained material has the chance to be another choice for applications on white LEDs combined with near-UV LED chips.

This work was supported by the National Natural Science Foundation of China (Grant Nos. 61275180 and 51472125) and the K.C. Wong Magna Fund of Ningbo University.

References

1. A. Bergh, G. Craford, A. Duggal, and R. Haitz, Phys. Today **54**, 42 (2001).
2. R. Cao, K. N. Sharafudeen, and J. Qiu, Spectrochim. Acta Part A **117**, 402 (2014).
3. N. M. Zhang, C. F. Guo, J. M. Zheng, X. Y. Su, and J. Zhao, J. Mater. Chem. C **2**, 3988 (2014).
4. C. K. Chang and T. M. Chen, Appl. Phys. Lett. **91**, 081902 (2007).
5. C. C. Chiang, M. S. Tsai, and M. H. Hon, J. Electrochem. Soc. **154**, J326 (2007).
6. D. Kang, H. S. Yoo, S. H. Jung, H. Kim, and D. Y. Jeon, J. Phys. Chem. C **115**, 24334 (2011).
7. S. Nishiura, S. Tanabe, K. Fujiok, and Y. Fujimoto, Opt. Mater. **33**, 688 (2011).
8. Z. F. Zhu, Y. B. Zhang, Y. P. Qiao, H. Liu, and D. G. Liu, J. Lumin. **134**, 724 (2013).
9. H. Y. Fu, X. S. Qiao, S. Cui, Q. Luo, J. Y. Qian, X. P. Fan, and X. H. Zhang, Mater. Lett. **71**, 15 (2012).
10. R. Bagga, V. G. Achanta, A. Goel, J. M. F. Ferreira, N. P. Singh, D. P. Singh, M. Falconieri, and G. Sharma, Mater. Sci. Eng. B **178**, 218 (2013).
11. R. Ye, Z. G. Cui, Y. J. Hua, D. G. Deng, S. L. Zhao, C. X. Li, and S. Q. Xu, J. Non-Cryst. Solids **357**, 2282 (2011).
12. T. Jiang, X. Yu, X. Xu, H. Yu, D. Zhou, and J. Qiu, Chin. Opt. Lett. **12**, 011601 (2014).
13. X. Y. Liu, Y. L. Wei, and H. Guo, J. Am. Ceram. Soc. **96**, 369 (2013).
14. G. Lakshminarayana, H. C. Yang, and J. R. Qiu, J. Solid State Chem. **182**, 669 (2009).
15. L. Tang, H. Xia, P. Wang, J. Peng, and H. Jiang, Chin. Opt. Lett. **11**, 061603 (2013).
16. N. Vijaya, K. U. Kumar, and C. K. Jayasankar, Spectrochim. Acta A **113**, 145 (2013).
17. R. Rajeswari, C. K. Jayasankar, D. Ramachari, and S. S. Babu, Ceram. Int. **39**, 7523 (2013).
18. J. Y. Qian, Q. Luo, D. L. Zhao, S. Cui, X. S. Qiao, X. P. Fan, and X. G. Zhang, Opt. Mater. **34**, 700 (2012).